Theoretical Prediction and Experimental Verification of Multiple Steady States for Parametric Roll

Gabriele Bulian (gbulian@units.it) & Alberto Francescutto (francesc@units.it)

Dept. of Naval Architecture, Ocean and Environmental Engineering, Univ. of Trieste, Trieste, Italy

ABSTRACT

The paper reports a series of analytical predictions, together with experimental verification, of the coexistence of multiple steady states for parametrically excited rolling motion in the first parametric resonance region in longitudinal regular waves. A stable resonant solution can coexist with a stable upright position, as well as with other stable resonant solutions with finite amplitude. The paper shows that stable rolling motions can occur outside the linear Mathieu instability region, and that the peak of the response curve is not rarely outside the linear Mathieu instability region. A numerical measure, defined here the "attraction index", has been introduced to decide on the "relative importance" of different attractors, and this measure could be useful when direct time domain numerical simulations of parametric roll are used in a regulatory framework.

KEYWORDS

nonlinear parametric roll; multiple steady states; attraction domains;

INTRODUCTION

Research concerning the parametrically excited rolling motion has, in recent years, significantly grown. As a consequence, the level of knowledge about the phenomenon in the international community has significantly increased. Nevertheless it seems that a typical nonlinear effect, namely the coexistence of multiple steady states under regular sea excitation, has not yet received a wide attention. Developments concerning Classification Societies' rules (ABS , 2004) and the present IMO-SLF work towards the creation and implementation of performance based criteria specifically addressing parametric roll are calling for a deeper understanding of the quite subtle issues that could be associated, in the framework of the approval of simulations/experiments, with the presence of coexisting multiple steady states (IMO, 2005). The presence of multiple steady states under parametric excitation seems to be a known possibility since long ago (see, e.g., the response curves reported by Grim (1952)) and also more recently, analytical approaches have shown such possibility (Spyrou, 2005). In literature it is possible to find the numerical evidence of possible multiple steady states, as, e.g., in the application of a 3-DOF model by Neves & Rodríguez (2007), where the simulated steady state rolling amplitude was shown to be dependent on the initial conditions in some range of waves and ship speeds. In (Umeda et al., 2003 ; Hashimoto & Umeda, 2004) time domain numerical simulations of a nonlinear 1-DOF parametric roll model showed the possible coexistence of a stable upright position and a resonant solution in some ranges of parameters. A similar outcome can be found in the numerical simulations reported by Bulian (2005). In other published cases, such as in numerical results shown by France et al. (2003–fig.25 and fig.30) or by Shin et al. (2004-fig. 45), the presence of sudden jumps in the roll response curve suggest the presence of fold bifurcations, and, as a consequence, the possible presence of coexisting steady states. Nevertheless, in recent time there seems to have been very few experiments specifically devoted to the identification of multiple attractors (see, e.g., Oh et al. (2000)). At the same time, the ITTC procedures for parametric roll (ITTC, 2006) implicitly address the presence of multiple steady states when providing the analytical solution of the steady rolling amplitude for a nonlinear 1-DOF model.

In this paper we deal with the theoretical prediction and the experimental verification of the presence of different steady states for the parametrically excited rolling motion of two RoRo ships. An analytical 1-DOF model is used in order to disclose the possible presence of coexisting attractors, and to show that the shape of the roll response curve can significantly differ from ship to ship and from condition to condition. Experimental results are also reported: in one case we confirm the coexistence of a stable upright condition together with a resonant, stable, large amplitude solution, while a second experimental case shows the coexistence of two non-trivial stable solutions associated to different rolling amplitudes. In order to address the problem of the "relative importance" of coexisting attractors, an index is finally introduced based on data obtained from the topology of the space of initial conditions. The index is then applied to a series of numerical data.

THEORETICAL MODEL

In the study of parametric roll in longitudinal waves we can find basically three approaches (others are slight modifications of the reported three):

- A fully numerical approach, able, in principle, to address the problem taking into account all the necessary coupling between motions (e.g. France et al. (2003), Shin et al. (2004)). In this approach the problem is addressed in time domain only.
- A 3-DOF analytical model for roll, heave and pitch (e.g. Neves & Rodríguez (2007)). In this case the equations of motions are fully analytic. The stability boundaries for the loss of stability of the upright position are determined analytically in approximate form, however the amplitude of motions are determined by time domain simulations, since an analytical approach with 3-DOF for the steady state amplitude of motions is mostly prevented by the complexity of the system of equations.
- A 1-DOF analytical model for roll (e.g. Francescutto (2001), Bulian (2004, 2005, 2006a), Umeda et al. (2007), Spyrou (2005)). Of course this is the most basic model, but it allows obtaining reasonable indications concerning the inception and amplitude of parametric roll. Using a 1-DOF approach, it is possible to determine analytically, although in an approximate way, both the instability region and, to some extent, the steady state amplitude of roll.

In this work we are interested in analysing the problem of the presence of multiple steady states in longitudinal regular waves more qualitatively than quantitatively, and for this reason we use a 1-DOF approach based on Bulian, (2004, 2006a), where the steady state rolling amplitude is determined analytically in an approximate way in the first parametric resonance region together with the stability properties of each solution by using the averaging technique.

The analytical approach starts from the following 1-DOF equation for the roll motion in longitudinal regular waves (that is also consistent with ABS (2004)):

$$\ddot{\phi} + d\left(\phi,\dot{\phi}\right) + \omega_0^2 \cdot \frac{\overline{GZ}\left(\phi, x_c \middle| a_w, \lambda\right)}{\overline{GM}} = 0 \qquad (1)$$

where $d\left(\phi,\dot{\phi}\right)$ is the damping function, ω_0 is the roll natural frequency in calm water, $\overline{GM}$ is the calm water metacentric height, and $\overline{GZ}\left(\phi, x_c\right)$ is the righting lever depending on the roll angle ϕ and the position x_c of the wave crest along the ship. It is to be noted that equation (1) is considered for a given wave amplitude a_w and wave length λ. By performing (Bulian (2005, 2006a)) a polynomial fitting of $\overline{GZ}\left(\phi, x_c \middle| a_w, \lambda\right)$ accounting for symmetry, and assuming a quite general linear+quadratic+cubic speed dependent model for the damping function it is possible to get the following fully analytical equation:

$$\ddot{\phi} + 2\mu(V)\cdot\dot{\phi} + \beta(V)\cdot\dot{\phi}\left|\dot{\phi}\right| + \delta(V)\cdot\dot{\phi}^3 + $$
$$+\frac{\omega_0^2}{\overline{GM}}\cdot\begin{bmatrix}\overline{GZ}_{ave}\left(a_w,\lambda,\phi\right)+ \\ +\delta\overline{GZ}\left(a_w,\lambda,\phi,t\right)\end{bmatrix} = 0$$

$$\overline{GZ}_{ave}\left(a_w,\lambda,\phi\right) =$$
$$= \sum_{j=1,3,5,\ldots,N_p} Q_{j0}\left(a_w,\lambda\right)\cdot\phi^j$$

$$\delta\overline{GZ}\left(a_w,\lambda,\phi,t\right) = \tag{2}$$
$$= \sum_{j=1,3,5,\ldots,N_p}\left(\sum_{n=1}^{N_h}\Psi_{jn}\left(a_w,\lambda,t\right)\right)\cdot\phi^j$$

$$\Psi_{jn}\left(a_w,\lambda,t\right) =$$
$$=\begin{bmatrix} Q_{jn}^c\left(a_w,\lambda\right)\cdot\cos\left(n\cdot\dfrac{\omega_e\cdot t}{\cos(\chi)}\right)+ \\ +Q_{jn}^s\left(a_w,\lambda\right)\cdot\sin\left(n\cdot\dfrac{\omega_e\cdot t}{\cos(\chi)}\right)\end{bmatrix}$$

where V is the ship speed, while the coefficients $Q_{jn}^{(..)}\left(a_w,\lambda\right)$ come from the polynomial fitting of $\overline{GZ}\left(\phi, x_c \middle| a_w, \lambda\right)$, the encounter frequency is ω_e, and the encounter angle, to be equal to either 180deg in head sea, or 0deg in following sea, is χ. The model (2) can be efficiently solved in time domain (Bulian (2005)), however in Bulian (2004, 2006a) an approximate solution of the steady roll amplitude for the model (2) is given when the degree N_p of the polynomial fitting is less or equal to 9 and the roll motion exhibits a sub-harmonic regime as it occurs in the first parametric resonance (i.e. close to $\omega_e \approx 2\cdot\omega_0\sqrt{Q_{j0}\left(a_w,\lambda\right)/\overline{GM}}$). The limitation concerning the maximum degree of the polynomial fitting of $\overline{GZ}\left(\phi, x_c \middle| a_w, \lambda\right)$ is introduced in Bulian (2004) to keep the complexity of analytical formulae reasonably low (the method can of course be extended to higher values of N_p). According to the referred analytical method, the steady state rolling amplitude A in the first parametric resonance region can be obtained as equal to zero (trivial solution) or as the positive "meaningful" (Bulian (2004, 2006a)) real roots of a 32nd-degree polynomial, i.e.:

$$N_p \le 9 \Rightarrow \sum_{h=0}^{32} P_h\cdot A^h = 0 \cup A = 0 \tag{3}$$

where the coefficients P_h are functions of the parameters of the model (2) and, in particular, of the ratio between the encounter frequency ω_e and the natural roll frequency ω_0. The analytical expressions for the coefficients P_h can be found in Bulian (2004, 2006a), where, in addition, it is also reported how to analyse the stability of the obtained steady state solutions. Summarising, according to the reported analytical method it is therefore possible to have a global, though approximate, nonlinear frequency domain analysis of the behaviour of the 1-DOF model (1) in the region of the first parametric resonance.

Since in the next section we will discuss only the presence of non-trivial multiple solutions, we want just to point out here that the symmetry of the equation (1) (or (2)) always leads to the presence of couples of symmetric solutions (Bulian (2006b)), i.e. if $\phi_+(t)$ is solution of (1) (or (2)), then also $\phi_-(t) = -\phi_+(t)$ is solution of (1) (or (2)), and both solutions are associated to the same rolling angle/speed/acceleration since

$\forall n \quad \left|\frac{d^n}{dt^n}\phi_-(t)\right| = \left|\frac{d^n}{dt^n}\phi_+(t)\right|$. Although the solutions $\phi_+(t)$ and $\phi_-(t)$ should be considered, from theoretical point of view, as associated to different attractors, they can be considered to be the "same" solution when the interest is only on the absolute values of rolling amplitudes/velocities/accelerations. The analytical method leading to (3) always (and correctly) predicts the presence of a solution together with its opposite counterpart, appearing as a 180deg phase shift in the response (Bulian (2006a)).

EXAMPLES OF APPLICATION OF THE METHOD AND EXPERIMENTAL RESULTS

The picture provided by the referred analytical approximate method allows showing that the nonlinear steady state rolling response could have quite different shapes, depending especially on the characteristics of the nonlinearities of the righting lever in waves (e.g. mainly softening or mainly hardening). In the following we report a series of examples of application, together with a comparison with experimental results. Two RoRo ships have been selected as sample cases, and a more thorough analysis, comprising other ships also, is reported in Bulian (2006a). The main data of the considered ships are shown in Table 1, and speed dependent damping coefficients have been obtained from the analysis of experimental roll decays (Bulian (2006a)). The ship named "ITACA" has been tested with bilge keels ("BK") and without bilge keels ("BH"). When calculating the righting lever $\overline{GZ}$ for the ship on the wave, free trim equilibrium has been considered using a hydrostatic pressure distribution below the free surface. In the reported figures, as a convention, positive values for the ship speed mean head sea cases, whereas following sea cases are reported as negative ship speeds. Some of figures also report a bounding box made by a dashed-dot thick line that bounds the region where the analytical method can be considered as reasonable. The upper horizontal line of this box corresponds to the maximum heeling angle used in the fitting of $\overline{GZ}$. The boundary vertical lines correspond to the speed region where the assumed sub-harmonic roll response can be considered reasonable, i.e. in a region of speeds giving $\omega_e \in [1.5, 2.5] \cdot \omega_0 \sqrt{Q_{j0}(a_w, \lambda)/\overline{GM}}$. An additional vertical solid line is reported at the speed corresponding to $\omega_e = 2 \cdot \omega_0 \sqrt{Q_{j0}(a_w, \lambda)/\overline{GM}}$.

As a first example, we report in Figure 1 a comparison between simulations and experiments for the ship ITACA-BH considering a wave having length equal to the ship length and wave steepness (ratio between wave height and wave length) equal to 1/50. We can see that the simulations predict a region of instability of the upright position in the range between approximately $U = 1.4 m/s$ and $U = 3.7 m/s$ in head sea: this is the region of instability that can be obtained by analysing the linear Mathieu equation as obtained from the linearization of the model (2). However, it is important to note that in a significantly large region of speeds, between about $U = 0 m/s$ and $U = 1.4 m/s$, the analytical model predicts the coexistence of a stable trivial solution (roll amplitude equal to zero), and a stable resonant solution. The analytical approach, in addition, predicts an unstable solution that extends between the fold bifurcation close to $U = 0 m/s$ up to the unstable pitchfork bifurcation at $U = 1.4 m/s$. The experimental results show a behaviour close to that predicted by the analytical method (just as a note, for this ship the predictions based on a fix trim calculation of $\overline{GZ}$ perform better (Bulian (2006a))). The low value of the experimental amplitude obtained for $U = 1.9 m/s$ is not clear, and could be due to some effect of wave reflection from the sides of the tank. What is important to note is that in the low speed region, both the analytical model and the experimental results show the coexistence of two competing attractors, associated with two different steady states: the zero amplitude solution and the resonant solution. In Figure 1 the exact 2:1 resonance is indicated by a vertical line: the bending of the response curve towards the region of low frequencies of encounter is due to the average softening behaviour of the righting lever.

In Figure 2 we report the experimental evidence of the presence of the predicted competing attractors. The initial perturbation is not sufficient to start the parametric roll phenomenon, but a second, stronger, perturbation moves the ship to the resonant attractor, where the motion sets stationary until a new perturbation is given to force the ship, again, to the stable zero amplitude solution. A final perturbation shows the possibility of a new jump to the resonant attractor.

The coexistence of a stable upright position, together with a stable resonant solution has also been predicted and experimentally verified for the ship TR2, as shown in Figure 3 and Figure 4: the behaviour is very similar to what has been observed for the RoRo ITACA.

The coexistence of a the trivial zero amplitude solution, together with a resonant stable solution is a characteristic that can be predicted also by the simplest nonlinear model for parametric roll, i.e. a model with time dependent metacentric height, and a constant, nonlinear cubic term in the restoring. However, when the nonlinear model for the righting arm in waves is complicated by increasing the degree of the fitting polynomial of $\overline{GZ}$ and/or by introducing fluctuations also in the nonlinear restoring terms, the complexity of the roll response curve can increase (Bulian (2006a,c)). In Figure 5 the results from experiments carried out on the ship ITACA fitted, now, with bilge keels are compared with analytical predictions. It is interesting that both the experiments and the analytical predictions show a reduction in the resonant branch of the response curve at low speed, with the shifting of the fold bifurcation predicted by the analytical method from approximately $U = 0m/s$ to approximately $U = 1.1m/s$. The modification of the response curve is mainly due to the additional damping provided by the bilge keels that reduces the resonant range (i.e. the region close to the fold bifurcation). A new interesting feature of the response curve is, however, now visible, i.e. the possible presence, in a limited range of speeds, of four coexisting attractors, namely the unstable upright position, a stable resonant solution with low amplitude, an unstable finite amplitude solution, and a large amplitude resonant stable solution. The range of speeds where this situation is predicted by the analytical model is very small, i.e. approximately in the interval $U \in [1.29,1.30]m/s$, and it starts with a stable pitchfork bifurcation in the low speed side, where the upright position loses its stability, and a finite amplitude stable solution is created. The region of coexistence ends with a fold bifurcation that destroys the low amplitude resonant solution. The experiments have verified the predicted coexistence of two finite amplitude stable solutions, although the speed at which this coexistence has been found is slightly different from the region predicted by the 1-DOF model. Results from experiments are shown in Figure 6.

The type of response curves that can be predicted by using the model (2) can be quite complex, as in the example reported in Figure 7. The response curve predicted by the analytical method shows two stable pitchfork bifurcations as limits of the instability region for the upright position. In addition, a strong folding of the response curve occurs in the region between $U = 1.5m/s$ and $U = 2.4m/s$, where two resonant stable solutions coexist, together with an unstable upright position and an unstable large amplitude solution. Although the predictions and the experimental results are not very close, it seems that the complexity in the shape of the predicted response curve is reflected by the complexity in the shape of the experimental response curve. It is also to be said that the experimental points reported in Figure 7 come from an experimental campaign (Francescutto (2002)) that was carried out well before the development of the analytical approach reported in this paper, and therefore the possible coexistence of multiple steady states was not investigated with particular attention at that time.

THE "RELATIVE IMPORTANCE" OF DIFFERENT STEADY STATES

In the previous section we have shown that the possible presence of coexisting steady states not only can be, to some extent, predicted, but it can also be experimentally verified. The question now is how to deal with this feature that seems to be more common than expected. Unfortunately we cannot provide a definite answer, but we can provide some additional insight into the topology of the domains of attraction, in order to show that the "relative importance" of each solution can be different depending on the speed of advance, and we can propose a "measuring index" that could be useful in deciding which attractor is the "most important". Here with "relative importance" we refer, basically, to a sort of "likelihood", or better "chance" for the system to be captured by one attractor instead of another one.

We start in Figure 8 with the analytical approximate response curve for the ship ITACA in bare hull condition when the wave has a length equal to the ship length and the wave steepness is 1/50. The righting arm in waves is calculated using a fix trim approach. The analytical approximate solution predicts, in this case, a region of coexistence of a stable upright position and a stable resonant solution between $U = 0.61 m/s$ and $U = 1.27 m/s$. At $U = 1.27 m/s$ a stable pitchfork bifurcation occurs, the upright position loses its stability, and a small amplitude stable solution is borne that coexists with the stable large amplitude resonant solution that was present also in the low speed range. However, the small amplitude stable solution is soon destroyed by the fold bifurcation occurring approximately at $U = 1.31 m/s$. For higher speeds only one stable solution remains, together with an unstable upright position, up to $U = 3.65 m/s$ where another stable pitchfork bifurcation closes the instability region.

The used analytical method, however, cannot give information on the shape of the domains of attraction associated to each different stable solution. To obtain a deeper understanding on the topology of the domains of attraction for each different solution, we have performed a series of numerical time domain simulations of the model (2), and the results are summarised in Figure 9. The figure reports the numerically determined steady state rolling amplitude in a limited range of ship speeds. We can see that the analytical results are confirmed by the numerical simulations. For a series of five speeds, we have performed analyses of the attraction basins by systematically changing the initial conditions. It can be seen that, in the low speed range, before the fold bifurcation that destroys/creates the resonant stable steady state, all the initial conditions are associated to the trivial solution $\phi(t \to \infty) = 0$. As the ship speed is increased above the speed associated to the fold bifurcation, a domain of attraction for the resonant steady state is created that enlarges as the ship speed is increased, while the domain of attraction for the trivial solution shrinks. It is noteworthy that the safe basin, i.e. the zone of initial conditions not leading to capsize, remains almost constant. Close to the pitchfork bifurcation the majority of initial conditions already belong to the attractor of the large amplitude resonant solution. When the speed is further increased above the speed corresponding to the low amplitude fold bifurcation, the upright position loses stability, and the whole safe basin now belongs to the resonant steady state's attractor.

According to the results reported in Figure 9, it can be seen that the "relative importance" of the large amplitude solution increases as the ship speed is increased in head sea, and, conversely, the "relative importance" of the solution $\phi = 0$ decreases. This behaviour of the system should be borne in mind when performing and/or analysing numerical simulations. The peak of the response curve in Figure 9 occurs, indeed, at a speed where the "relative importance" of the resonant solution is significantly smaller than the "relative importance" of the trivial solution, whereas the "relative importance" of the two attractors becomes the same at higher speed, where the resonant solution shows a smaller amplitude. In case a nonlinear model like (1) or (2) is used to determine to what extent the ship is prone to show parametric roll (e.g. ABS (2004)), it could be important to give some attention to the domains of attractions associated to possible different coexisting solutions in order to avoid too conservative decisions.

However, it is necessary, from an engineering point of view, to associate some numerical measure to each attractor in order to have a means for comparing their, so far referred but not clearly defined, "relative importance". Here we propose to use an index, named "attraction index" that is a measure of the "quantity" of initial conditions leading to a given attractor, normalised with respect to the extent of the safe basin. Given the generic j-th attractor, a general definition of this index could be given as follows:

$$AI_j = \frac{\int_{-\infty}^{\infty} \dots \int_{-\infty}^{\infty} I_j\left(\underline{x}\right) \cdot f\left(\underline{x}\right) dx_1 dx_2 \dots dx_N}{\int_{-\infty}^{\infty} \dots \int_{-\infty}^{\infty} I_{sb}\left(\underline{x}\right) \cdot f\left(\underline{x}\right) dx_1 dx_2 \dots dx_N} \tag{4}$$

$$\underline{x} = \left(x_1, x_2, .., x_N\right)$$

where:

- $\underline{x} = \left(x_1, ..., x_N\right)$ is the vector of the initial condition in the space of state parameters;
- $I_{sb}\left(\underline{x}\right)$ is the indicator function for the safe basin, depending on the initial condition $\underline{x}$, that is equal to 1 for initial conditions not leading to capsize, and 0 for initial conditions leading to capsize;
- $I_j\left(\underline{x}\right)$ is the indicator function for the j-th attractor, depending on the initial condition $\underline{x}$, that is equal to 1 for initial conditions leading to the j-th attractor, and 0 otherwise;
- $f\left(\underline{x}\right)$ is a generic weighting function, and it can be used to take into account, e.g., that different initial conditions have different likelihood of occurrence, and in this latter case it can be interpreted as a joint probability density function for the elements of the vector of initial conditions.

In the case of our 1-DOF model the state space is two dimensional, and so it is the vector of initial conditions $\underline{x} = \left(\phi_0 = \phi\left(t=0\right), \dot{\phi}_0 = \dot{\phi}\left(t=0\right)\right)$. If we assume a uniform weighting function $f\left(\underline{x}\right)$, equation (4) reduces to:

$$AI_j = \frac{\int_{-\infty}^{\infty} \int_{-\infty}^{\infty} I_j\left(\phi_0, \dot{\phi}_0\right) d\phi_0 d\dot{\phi}_0}{\int_{-\infty}^{\infty} \int_{-\infty}^{\infty} I_{sb}\left(\phi_0, \dot{\phi}_0\right) d\phi_0 d\dot{\phi}_0} \tag{5}$$

According to (5), we have determined the attraction indices for the stable large amplitude and low amplitude solution according to the numerical data reported in Figure 9, and results are shown in Figure 10: it can be seen that the introduced measure AI_j allows to decide that the large amplitude attractor is to be considered "more important" than the low amplitude attractor for speeds above approximately $U = 0.96 m/s$. For $U > 0.96 m/s$, indeed, the attraction index for the large amplitude attractor is larger than the attraction index for the low amplitude attractor.

Of course this result in Figure 10 is strongly dependent on the selection of the weighting function $f\left(\underline{x}\right)$ in (4). According to common sense, it could be more sound to select a weighting function giving more importance to initial conditions close to an "average" condition $\left(\bar{\phi}, 0\right)$, being $\bar{\phi}$ an average heel angle obtained by considerations outside the modelling (1),(2). A typical suitable weighting function could be, but is absolutely not limited to, a joint Gaussian distribution for roll motion and roll velocity. To some extent this idea reminds, or can be connected, to past works on critical wave episodes (Blocki (1980,1994)) or on the determination of the capsize risk in following sea (Umeda & Yamakoshi (1993)).

FINAL REMARKS

In this paper we have reported a series of analytical predictions, together with experimental verification, of the fact that the parametrically excited rolling motion in the first parametric resonance region in longitudinal regular waves could be characterised (more usually than expectable according to past available literature) by the presence of coexisting attractors associated to different steady states. We have shown that, due to the nonlinearities of the restoring, stable rolling motions can occur outside the linear Mathieu instability region and that these motions can coexist with a stable upright position. We have also shown that the type of bifurcations bounding the instability region for the upright position can be either stable or unstable pitchforks, depending on the nonlinearities of the restoring. In case of softening restoring a stable pitchfork bifurcation in the low encounter frequency side of the Mathieu instability zone can also lead to the coexistence of multiple stable solutions associated to finite amplitudes. Although not shown in this paper, it is likely that a similar situation could occur close to the high encounter frequency side of the Mathieu instability range for ships having hardening restoring, as often occurs for containerships. We have also shown the possible theoretically predicted, but not experimentally verified, coexistence of multiple finite amplitude steady states inside the Mathieu instability region. A numerical measure, defined here the “attraction index”, has been introduced to decide on the “relative importance” of different attractors: this could be an important issue when direct time domain numerical simulations of parametric roll are used in a regulatory framework. As a side outcome of our analyses, we have shown that the peak of the roll response curve in the first parametric resonance region is almost invariably predicted far from the exact 2:1 when waves are large enough to render the effect of nonlinearities of restoring significant. In particular, the peak of the roll response curve can occur at a ship speed that is outside the linear Mathieu instability region, in competition with a stable upright position.

REFERENCES

American Bureau of Shipping (ABS), (2004) "Guide for the assessment of parametric roll resonance in the design of container carriers", December.

Blocki, W., (1980) “Ship Safety in Connection with Parametric Resonance of the Roll”, International Shipbuilding Progress, Vol. 27, 1980, pp. 36-53.

Blocki, W., (1994) “Ship’s Stability Safety in Resonance Case”, Proc. 5th International Conference on Stability of Ships and Ocean Vehicles (STAB’94), Melbourne, Florida, 1994.

Bulian, G., (2004) “Approximate Analytical Response Curve for a Parametrically Excited Highly Nonlinear 1-DOF System with an Application to Ship Roll Motion Prediction”, Nonlinear Analysis: Real World Applications, Vol. 5, No. 4, September 2004, pp. 725-748. doi:10.1016/j.nonrwa.2004.03.002

Bulian, G., (2005) “Nonlinear Parametric Rolling in Regular Waves - A General Procedure for the Analytical Approximation of the GZ Curve and Its Use in Time Domain Simulations”, Ocean Engineering, Vol 32, No. 3-4, March, pp. 309-330. doi:10.1016/j.oceaneng.2004.08.008.

Bulian, G., (2006a) "Development of analytical nonlinear models for parametric roll and hydrostatic restoring variations in regular and irregular waves", Ph.D. Thesis, DINMA – University of Trieste, March. (http://hdl.handle.net/10077/2518).

Bulian, G., (2006b) "Experimental investigation on parametric roll in longitudinal irregular waves for a partially restrained post-panamax containership", Technical Report - JSPS Fellowship PE05052, Dept. of Naval Architecture and Ocean Engineering, Osaka University,.

Bulian, G., (2006c) "Nonlinear Parametric Rolling in Regular Waves - An Approximate Analytical Solution for the Response Curve in the Region of First Parametric Resonance", Journal of Ship Research, Vol. 50, No. 3, September, pp. 239-249.

France, W. N., Levadou, M., Treakle, T. W., Paulling, J. R., Michel, R. K., Moore, C., (2003) "An Investigation of

Head-Sea Parametric Rolling and Its Influence on Container Lashing Systems", Marine Technology, Vol. 40, pp. 1-19.

Francescutto, A., (2001) "An experimental investigation of parametric rolling in head waves", Transactions of the Association of Mechanical Engineers, Journal of Offshore Mechanics and Arctic Engineering, Vol. 123, pp.65–69.

Francescutto, A., (2002) "Theoretical Study of the Roll Motion in Longitudinal Waves", Technical Report (in Italian), Dept. DINMA, University of Trieste, 2002.

Grim, O., (1952) "Rollschwingungen, Stabilität und Sicherkeit im Seegang", Schiffstechnik, Vol. 1, pp. 10-21.

Hashimoto, H., Umeda, N., (2004) "Nonlinear analysis of parametric rolling in longitudinal and quartering seas with realistic modeling of roll-restoring moment", Journal of Marine Science and Technology, Vol. 9, 2004, pp. 117-126. doi:10.1007/s00773-004-0184-8

IMO Document SLF48/4/12, (2005) "On the development of performance-based criteria for ship stability in longitudinal waves", Submitted by Italy, 11 July.

International Towing Tank Conference (ITTC), (2006) "ITTC – Recommended Procedures and Guidelines - Predicting the Occurrence and Magnitude of Parametric Rolling (7.5-02-07-04.3)", (downloadable from http://ittc.sname.org/documents.htm)

Neves, M.A.S., Rodríguez, C.A., (2007) "Nonlinear Aspects of Coupled Parametric Rolling in Head Seas", Proc. 10th International Symposium on Practical Design of Ships and Other Floating Structures, Houston, 2007.

Oh, I.G., Nayfeh, A.H., Mook, D.T., (2000) "A theoretical and experimental investigation of indirectly excited roll motion in ships", Philosophical Transactions of the Royal Society, Mathematical, Physical and Engineering Sciences 358, pp.1853–1881.

Shin, Y.S., Belenky, V.L., Paulling, J.R., Weems, K.M., Lin, W.M., (2004) "Criteria for Parametric Roll of Large Containerships in Longitudinal Seas", Presented at the SNAME Annual Meeting in Washington, DC, 30 September.

Spyrou, K.J., (2005) "Design criteria for parametric rolling", Oceanic Engineering International, Ocean Engineering Internationa, Vol. 9, No. 1, pp. 11-27

Umeda, N., Hashimoto, H., Minegaki, S., Matsuda, A., (2007) "Preventing Parametric Roll with Use of Devices and Their Practical Impact", Proc. 10th International Symposium on Practical Design of Ships and Other Floating Structures, Houston, 2007.

Umeda, N., Hashimoto, H., Vassalos, D., Urano, S., Okou, K., (2003) "Nonlinear Dynamics on Parametric Roll Resonance with Realistic Numerical Modelling", Proc. 8th International Conference on Stability of Ships and Ocean Vehicles (STAB2003), Madrid, September, pp. 281-290

Umeda, N., Yamakoshi, Y., (1993) "Probability of Ship Capsizing due to Pure Loss of Stability in Quartering Seas", Selected Papers from the Society of Naval Architects of Japan 30, pp. 73-85

Table 1: Main data of the sample ships at full scale.

Ship	Length [m]	Breadth [m]	Draught [m]	Hull Volume [m^3]	Metacentric height [m]	Roll period at zero speed [s]	Trim [m]	Model scale
TR2	132.22	19.0	5.875	7714	0.865	15.9	0	1:50
ITACA	52.55	10.0	2.100	569	1.057	9.0(BH) 9.2(BK)	0	1:30

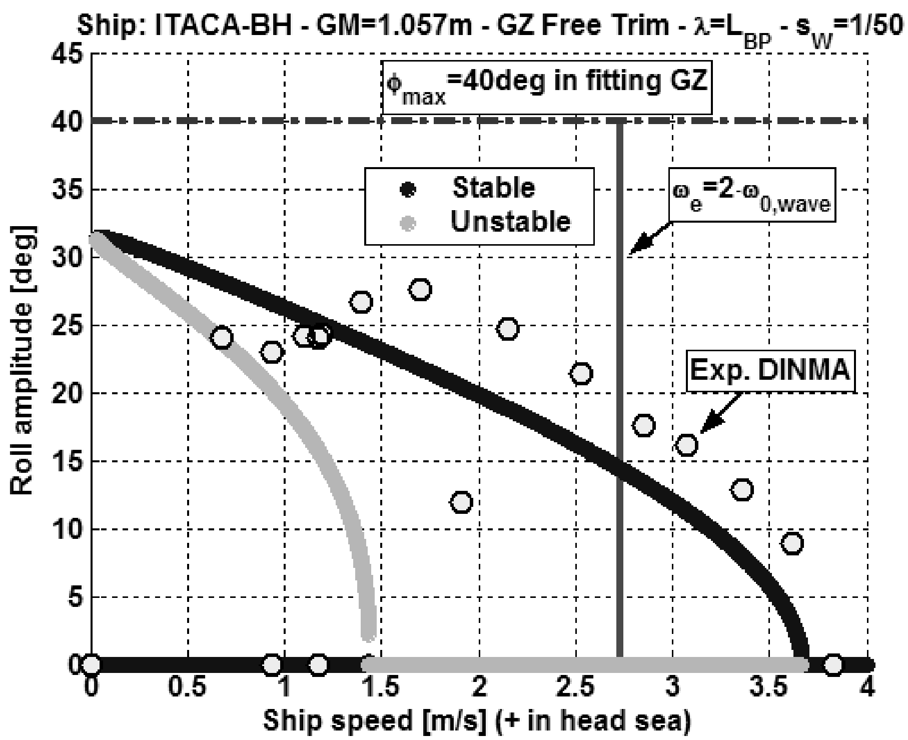

Figure 1: Experimental results and prediction for ITACA-BH, $\lambda / L = 1.0$ and $H / \lambda = 1/50$. Free trim calculation of $\overline{GZ}$ surface.

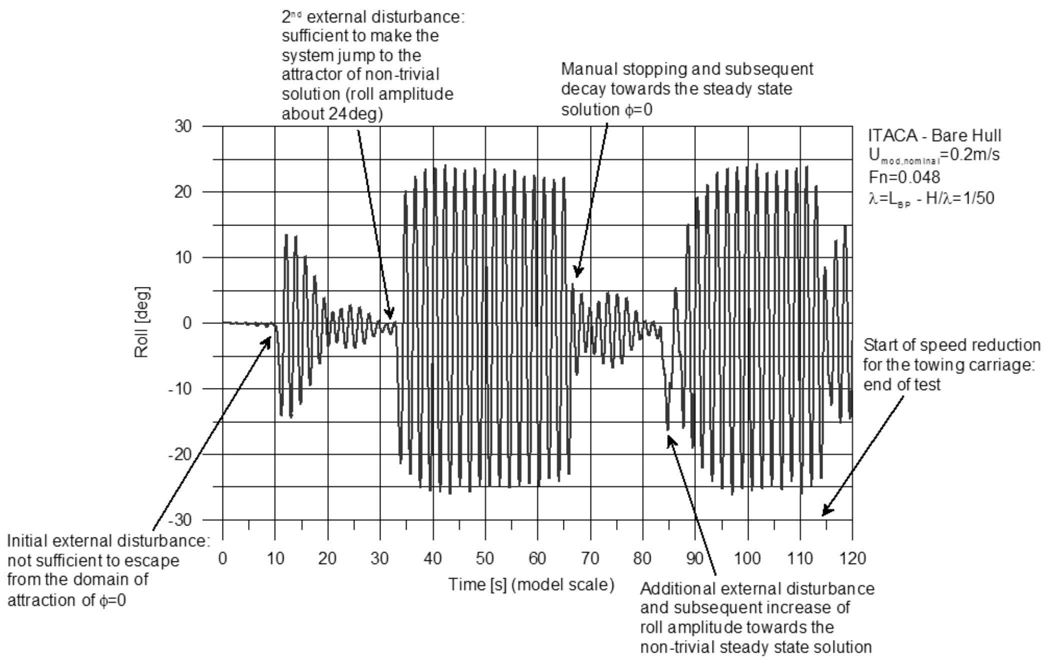

Figure 2: Experimental time series showing the presence of a stable upright position together with a stable large amplitude sub-harmonic resonant roll motion for ITACA-BH.

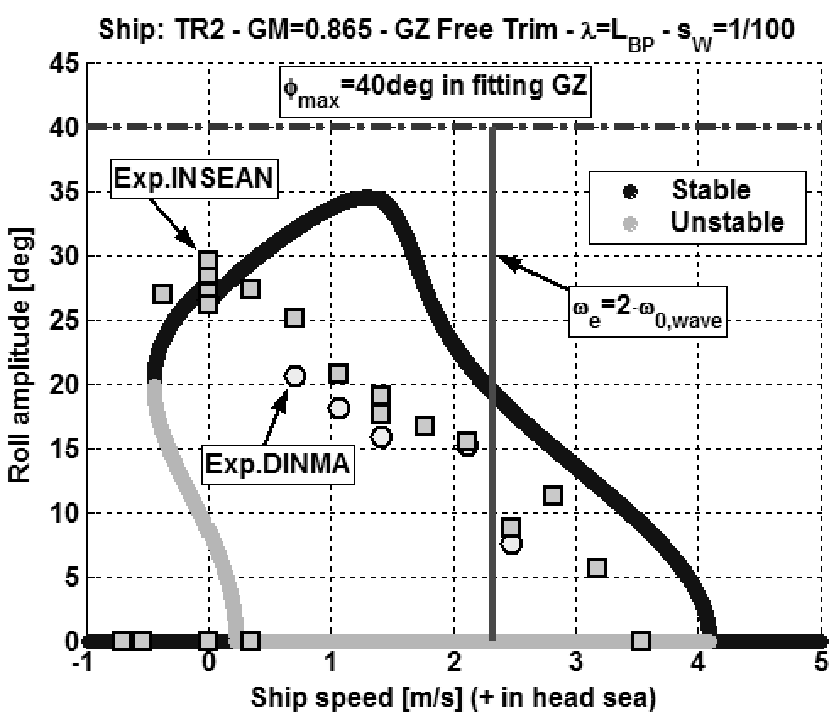

Figure 3: Experimental results and prediction for TR2, $\lambda / L = 1.0$ and $H / \lambda = 1/100$. Free trim calculation of $\overline{GZ}$ surface.

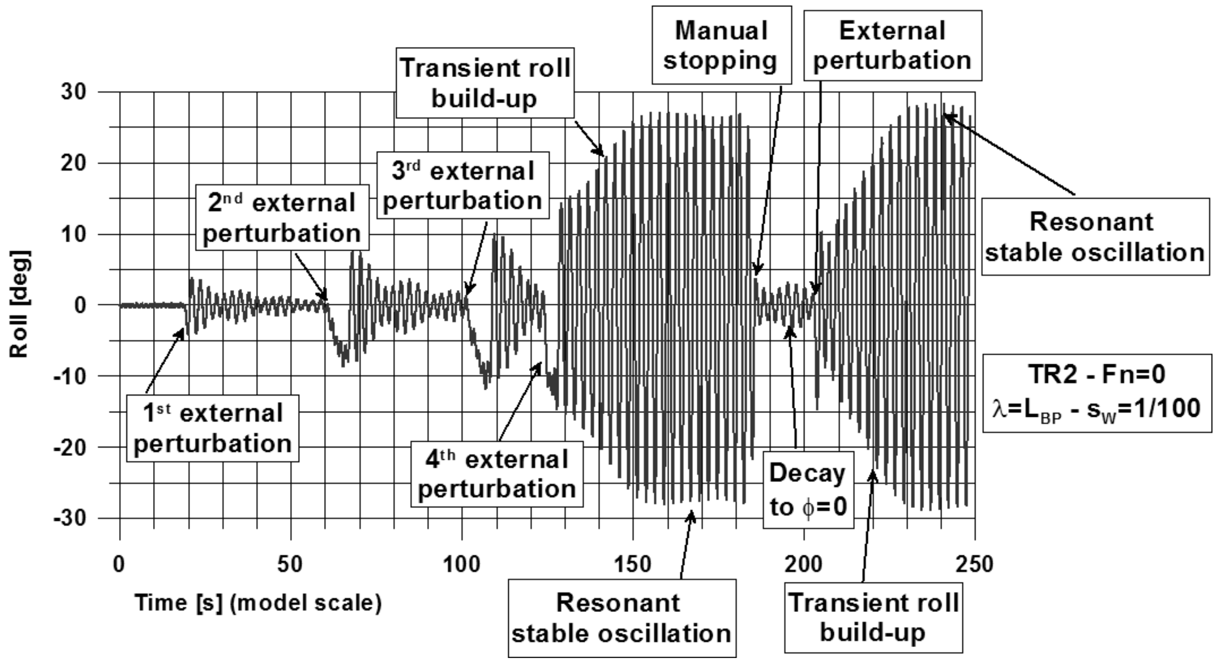

Figure 4: Experimental time series showing the presence of a stable upright position together with a stable large amplitude sub-harmonically resonant roll motion for TR2.

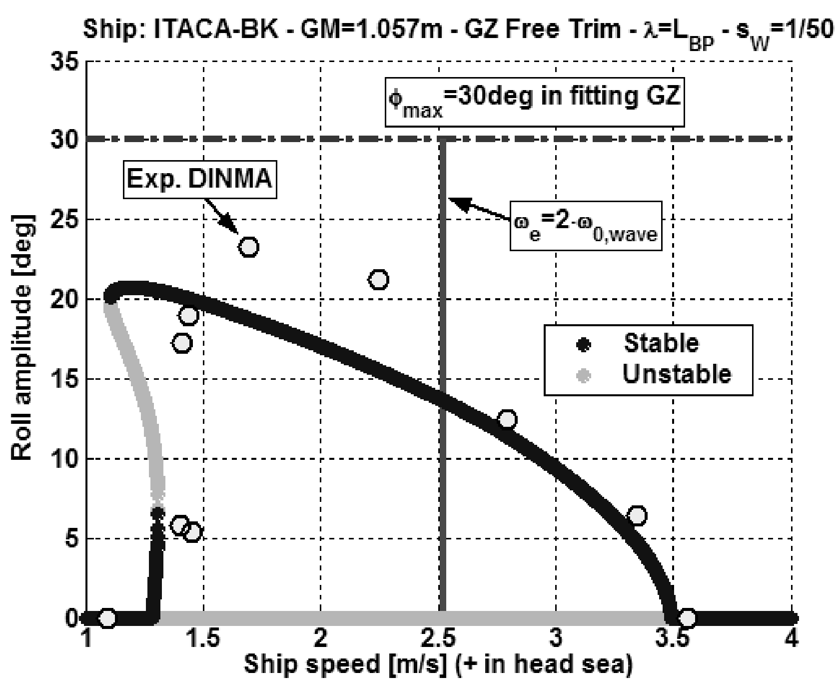

Figure 5: Experimental results and prediction for ITACA-BK, $\lambda / L = 1.0$ and $H / \lambda = 1/50$. Free trim calculation of $\overline{GZ}$ surface.

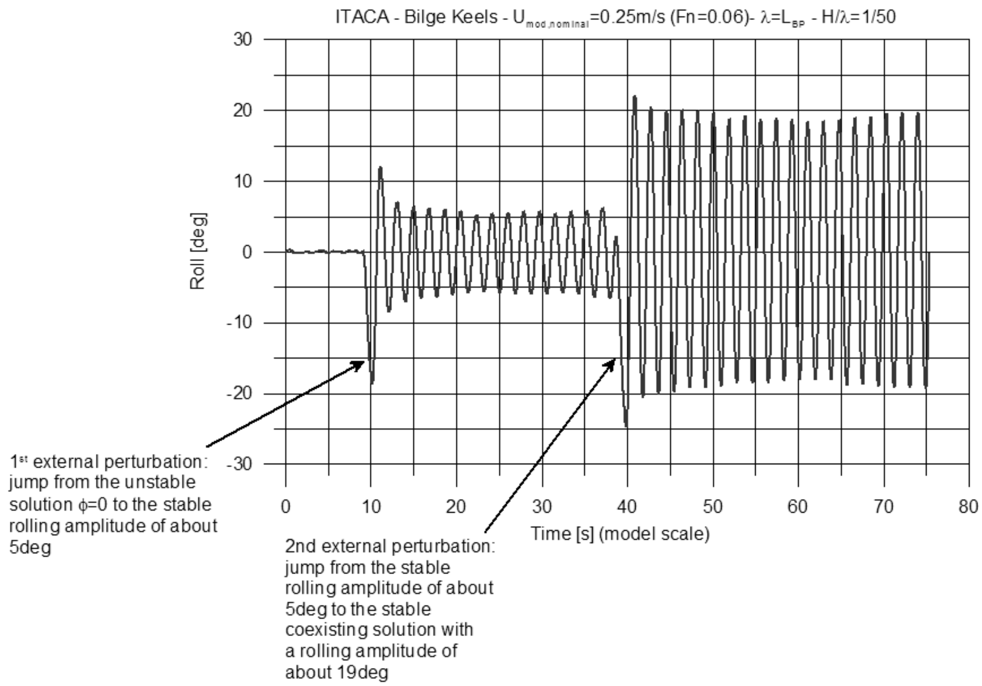

Figure 6: Experimental time series showing the presence of two stable non-zero amplitude solutions for the sub-harmonica resonant roll motion. ITACA fitted with bilge keels.

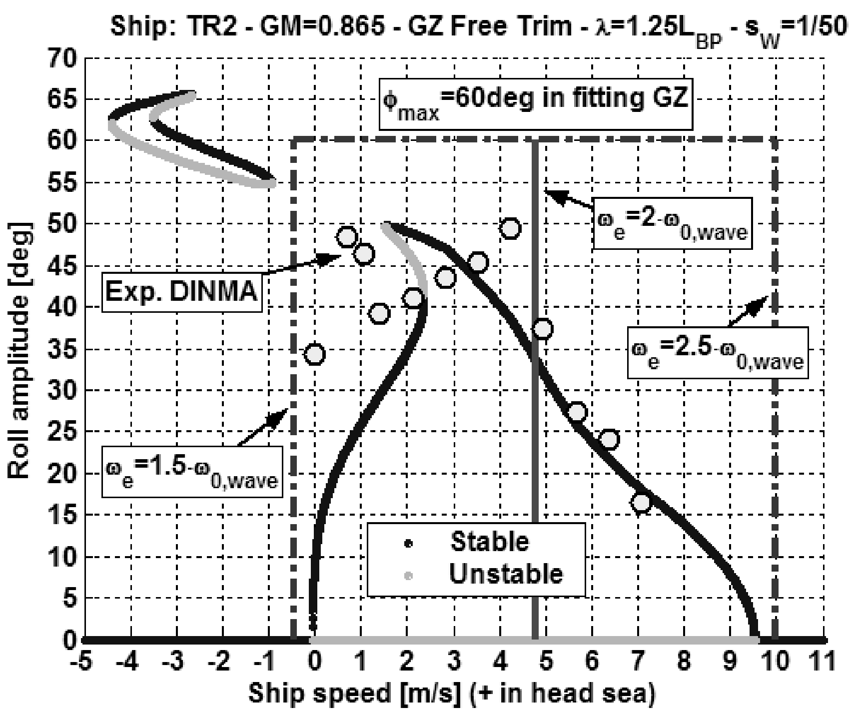

Figure 7: Experimental results and prediction for TR2, $\lambda / L = 1.25$ **and** $H / \lambda = 1/50$**. Free trim calculation of** $\overline{GZ}$ **surface.**

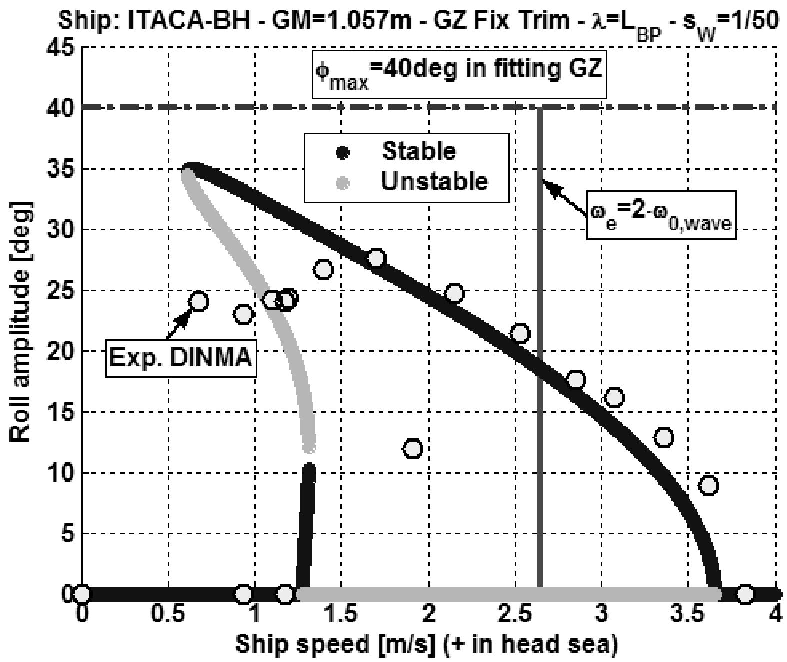

Figure 8: Experimental results and prediction for ITACA-BH, $\lambda / L = 1.0$ and $H / \lambda = 1/50$. Fix trim calculation of $\overline{GZ}$ surface.

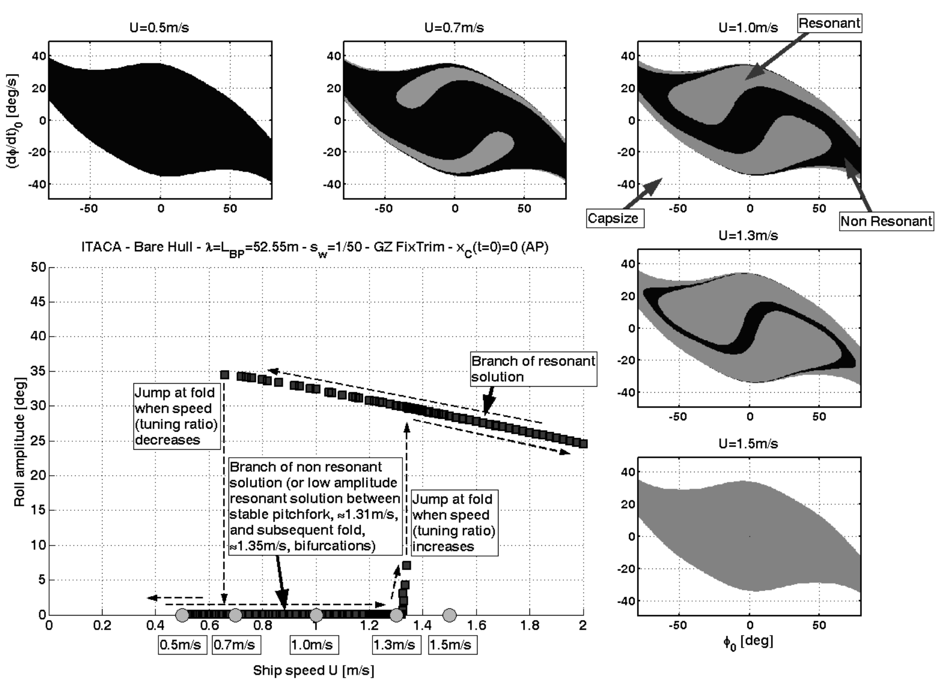

Figure 9: Analysis of domains of attraction. Ship ITACA-BH, $\lambda / L = 1.0$ and $H / \lambda = 1/50$. Fix trim calculation of $\overline{GZ}$ surface. Numerical integration of the 1-DOF model.

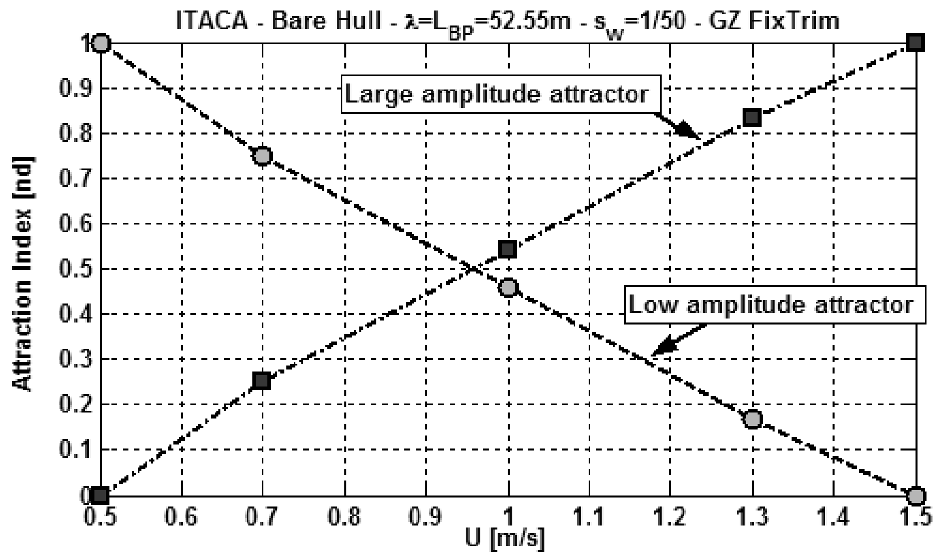

Figure 10: Analysis of the attraction index. Ship ITACA-BH, $\lambda / L = 1.0$ and $H / \lambda = 1/50$. Fix trim calculation of $\overline{GZ}$ surface. Numerical integration of the 1-DOF model.